Orbital Constraints on Exoplanet Habitability

Zachery McBrearty
Level 4 Project, MPhys Physics with Astronomy
Supervisor: Dr Richard Wilman
Second Supervisor: Dr Craig Testrow
Department of Physics, Durham University

Submitted: February 15, 2024

A 1-D energy balance climate model is developed in order to investigate how changing certain orbital parameters can result in changes to a planet's habitability. Theoretical relationships between temperature, semimajoraxis, and eccentricity are derived from a simple 0-D energy balance model and are tested against the 1-D model and are found to be correct. A qualitative analysis of obliquity shows that there are optimal obliquities to minimise and maximise global temperature. The climates of exomoons orbiting gas giants are also investigated, including reflected light from the gas giant, eclipsing, and tidal heating. It is expected that these additional sources of heat move the habitable zones for the planet outwards.

CONTENTS

1. Introduction 3

2. 1-D Energy Balance Climate Model 3
   A. Discretisation of the climate model 3

3. Method 4

4. Earth-like model 5

5. Earth-like exoplanets 9
   A. Investigating time-averaged solar flux 9
   B. Semimajor axis and eccentricity 11
   C. Obliquity 11
   D. Ocean fraction 11

6. Exomoons 11
   A. Eclipsing 11
   B. Tidal heating 16
   C. Developing and investigating a depth model 16

7. Discussion 16

8. Conclusion 16

References 16

A. Numerical stability of the 1D EBCM 19

B. Tidal heating equations and method 19

Scientific Summary for a General Audience 20

1. INTRODUCTION

$$\pi r^2 S(1-A) = 4\pi r^2 \sigma T^4, \tag{1}$$

$$C(\lambda, T)\frac{\partial T(t,\lambda)}{\partial t} = D\left[\frac{\partial^2 T(t,\lambda)}{\partial \lambda^2} - \tan\lambda \frac{\partial T(t,\lambda)}{\partial \lambda}\right] + S(\lambda,t)(1-A(T)) - I(T), \tag{2}$$

2. 1-D ENERGY BALANCE CLIMATE MODEL

The EBCM can be derived from the standard heat equation given by

$$\frac{\partial T}{\partial t} = \alpha \nabla^2 T, \tag{3}$$

where $T(t, r, \theta, \phi)$ is the temperature at time t, radius r, co-latitude θ, and longitude ϕ. The constant α is related to the heat capacity and diffusion rate of the system. Expanding the laplacian in spherical coordinates the equation becomes

$$\frac{\partial T}{\partial t} = \alpha\left[\frac{1}{r}\frac{\partial^2}{\partial r^2}(rT) + \frac{1}{r^2 \sin\theta}\frac{\partial}{\partial \theta}\left(\sin\theta \frac{\partial T}{\partial \theta}\right) + \frac{1}{r^2 \sin^2\theta}\frac{\partial^2 T}{\partial \theta^2}\right]. \tag{4}$$

The EBCM is arrived at by first letting $T(t, r, \theta, \phi) = T(t, \lambda)$, with latitude $\lambda = \pi - \theta$. Thus the equation simplifies to

$$\begin{aligned}\frac{\partial T}{\partial t} &= \frac{\alpha}{r^2 \sin\theta}\frac{\partial}{\partial \theta}\left(\sin\theta \frac{\partial T}{\partial \theta}\right) \\ &= \frac{\alpha}{r^2}\left(\frac{\partial^2 T}{\partial \lambda^2} - \tan\lambda \frac{\partial T}{\partial \lambda}\right).\end{aligned} \tag{5}$$

The original equation can be recovered by defining $\alpha/r^2 \equiv D/C$ for diffusion constant D and heat capacity C. Then adding incoming solar radiation S (insolation), which is reduced by planetary albedo A, and outgoing IR-emission I to the PDE. Thus the original form of the 1D EBCM in eqn. (2) is recovered.

A. Discretisation of the climate model

Numerically integrating the EBCM requires the derivatives to be discretised. Spatially the planet can be split into S latitude bands, separated by

$$\Delta\lambda = \frac{\pi^{\text{rad}}}{S-1} = \frac{180°}{S-1}, \tag{6}$$

with spatial indexing of each band from $m = 0, 1, \dots, S-1$. Similarly, a temporal indexing of $n = 0, 1, \dots$ is used to discretise time in steps of Δt. Thus T_n^m is the temperature at the m^{th} timestep for the n^{th} latitude band.

The spatial derivatives can then be approximated by the central difference and second order central difference:

$$\frac{\partial T_n^m}{\partial \lambda} = \frac{T_n^{m+1} - T_n^{m-1}}{2\Delta\lambda}, \tag{7}$$

$$\frac{\partial^2 T_n^m}{\partial \lambda^2} = \frac{T_n^{m+2} - 2T_n^m + T_n^{m-2}}{(2\Delta\lambda)^2}, \tag{8}$$

and the temporal derivative can be approximated as a forward difference,

$$\frac{\partial T_n^m}{\partial t} = \frac{T_{n+1}^m - T_n^m}{\Delta t}, \tag{9}$$

with numerical stability analysed in appendix A. Evolving the EBCM is performed by solving eqn. (9) for T_{n+1}^m in terms of the parameter and temperature values at timestep n.

However, a problem arises at the edges of the model as $m = -2, -1, S, S+1$ are not defined. To fix this the derivatives at $m = 0$ ($m = S-1$) are discretised as forward then backward (backward then forward) derivatives. By imposing that $\partial T_n^{m=0,S-1}/\partial\lambda = 0$, these second order derivatives reduce to

$$\frac{\partial^2 T_n^{m=0}}{\partial \lambda^2} = \left(\frac{\partial T_n^{m=1}}{\partial \lambda} - \frac{\partial T_n^{m=0}}{\partial \lambda}\right)/\Delta\lambda \qquad = \frac{T_n^{m=1} - T_n^{m=0}}{(\Delta\lambda)^2} \tag{10}$$

$$\frac{\partial^2 T_n^{m=S-1}}{\partial \lambda^2} = \left(\frac{\partial T_n^{m=S-1}}{\partial \lambda} - \frac{\partial T_n^{m=S-2}}{\partial \lambda}\right)/\Delta\lambda = \frac{T_n^{m=S-2} - T_n^{m=S-1}}{(\Delta\lambda)^2}. \tag{11}$$

Furthermore, the treatment imposed for the $m = 1$ and $m = S-2$ second order derivatives is much the same, using central-backward and central-forward derivatives respectively.

3. METHOD

Area averaging

$$\bar{Q}_n = \frac{\sum_{m=0}^{S-1} Q_n^m \cos(\lambda_m)\Delta\lambda}{\sum_{m=0}^{S-1} \cos(\lambda_m)\Delta\lambda}, \tag{12}$$

where $\lambda_m = m\Delta\lambda - \pi/2$ denominator evaluates to 2

Time averaging

$$\begin{aligned} Q_{p\to q}^m &= \frac{\sum_{n=p}^{q} Q_n^m \Delta t}{\sum_{n=p}^{q} \Delta t} \\ &= \frac{\sum_{n=p}^{q} Q_n^m}{q-p} \end{aligned} \tag{13}$$

where, since Δt is constant, the averaging over time becomes an average of a number of points.

total average

$$\bar{Q}_{p\to q} = \frac{\sum_{n=p}^{q} \sum_{m=0}^{S-1} Q_n^m \cos(\lambda_m)\Delta\lambda}{2(q-p)}, \tag{14}$$

which is simply the time and area averages of the temperature data

Semimajoraxis a, au	Eccentricity e	Obliquity δ, deg	No. spatial nodes S	Timestep Δt, days	Land fraction type
1	0.0167	23.5	61	1	Uniform 70% Ocean

TABLE I: A summary of the default parameters for the Earth-like model. A 'Uniform' land fraction indicates that the model has the same ratio of land to ocean across the entire planet. The odd number of spatial nodes means there is a true equator with $\lambda = 0$ as well as poles with $\lambda = \pm 90°$

The system is said to reach an equilbrium temperature when the average temperature between 2 averaging periods divided by the average temperature over both periods is less than some tolerance ϵ:

$$\frac{\bar{T}_{p\to q} - \bar{T}_{q\to r}}{\bar{T}_{p\to r}} < \epsilon, \tag{15}$$

typically the averaging occurs over an orbital period (i.e. local year), so the equilbrium temperature is when there are no significant variations in temperature between two consecutive orbits.

The classical habitability function is the Liquid Water Requirement (LWR) given by

$$H_{\text{LWR}}(T) = \begin{cases} 1 : 0°\text{C} \leq T \leq 100°\text{C} \\ 0 : \text{Otherwise} \end{cases}, \tag{16}$$

Thus a temperature is habitable if it is between the boiling and melting points of water.

An alternative is motivated by the limits of human endurance. If a human's core temperature is raised above $35°$C then enzymes esssential for life denature and breakdown. This does not mean temperatures above this are lethal as humans can regulate temperature by sweating. The wet bulb temperature is defined by wrapping a thermometer bulb with a wet cloth. It is designed to take the humidity and ambient temperature into account, essentially mimicking the internal temperature of a human. Thus a wetbulb temperature of $35°$C is lethal if prolonged.

This climate model does not calculate humidity, thus a conservative temperature at which habitability reduces is taken to be $30°$C:

$$H_{\text{HC}}(T) = \begin{cases} 1 : 0°\text{C} \leq T \leq 30°\text{C} \\ 0 : \text{Otherwise} \end{cases}, \tag{17}$$

with the additional constraint that temperatures greater than $40°$C or less than $-10°$C in a latitude band sets the habitability of the band to 0 for all time.

4. EARTH-LIKE MODEL

In order to investigate the Earth and Earth-like planets, the parameters and functions which define the Earth must be established. In this analysis the forms of the model functions are taken from Williams and Kastings (WK97) [2], and the model is compared against the model from North and Coakley 1979 (NC79) [1] which has been time-averaged as follows.

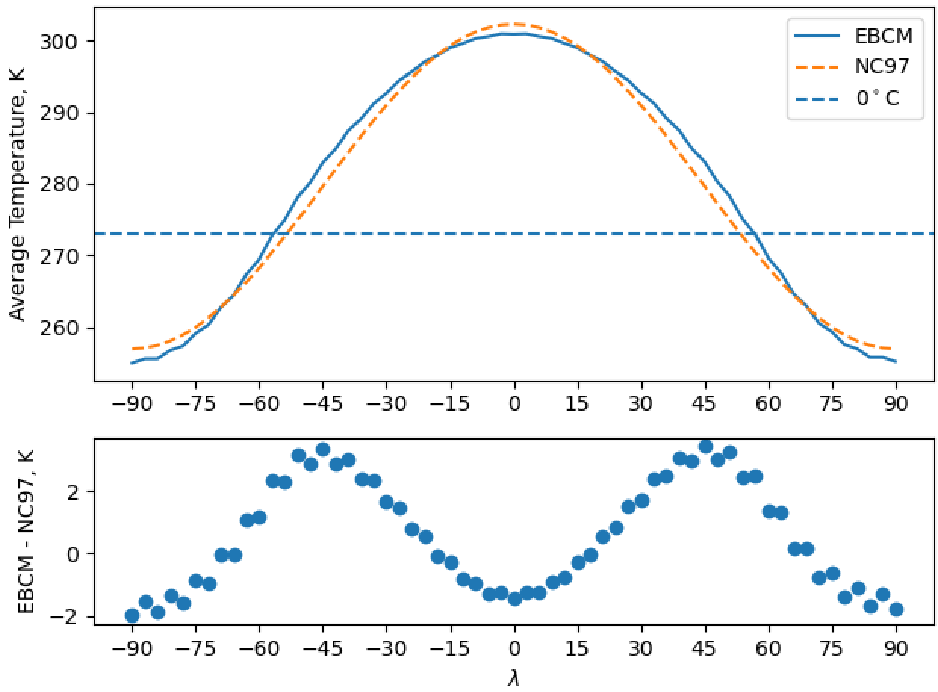

FIG. 1: The 10-year-averaged temperature distribution of the Earth-like model given in I. Overlaid on the fit is the time averaged Earth model from North and Coakley's 1979 paper [1]. The diffusion parameter D_0 in eqn. (20) was varied to give the best agreement between the two models. The value found to work best is $D_0 = 0.56\ \mathrm{Wm^{-2}K^{-1}}$.

The first 3 terms of the NC79 model are given in their eqn. (4) as

$$T(\lambda, t)[^\circ\mathrm{C}] = 14.2 + 15.5\cos(\omega t + \phi)P_1(\sin\lambda) - 30.2P_2(\sin(\lambda)), \tag{18}$$

where P_i is the i^{th} Legendre polynomial. The time-averaged temperature is found when averaging eqn. (18) over a year period,

$$\begin{aligned} T(\lambda)[\mathrm{K}] &= 14.2 + 273 - 30.2(3\sin^2(\lambda) - 1)/2 \\ &= 302.3 - 45.3\sin^2(\lambda), \end{aligned} \tag{19}$$

where the temperature has been converted to Kelvin, and the second legrendre polynomial is expanded as $P_2(x) = (3x^2 - 1)/2$. The average of $\cos(\omega t + \phi)$ over an period $T = 2\pi/\omega$ is 0, so the first legendre polynomial is not needed.

The diffusion varies with orbital and atmospheric parameters as,

$$\frac{D}{D_0} = \frac{p}{p_0}\frac{c_p}{c_{p,0}}\left(\frac{m}{28}\right)^{-2}\left(\frac{\Omega}{1\ \mathrm{day}^{-1}}\right)^{-2} \tag{20}$$

where $D_0 = 0.56\ \mathrm{Wm^{-2}K^{-1}}$ is from fitting to eqn. 19 as shown in Fig. 1. p is the atmospheric pressure relative to $p_0 = 101$ kPa. c_p is the heat capacity of the atmosphere, relative to $c_{p,0} = 1 \times 10^3\ \mathrm{g^{-1}K^{-1}}$. m is the (average) mass of the particles in the atmosphere, relative to the Nitrogen molecule. Ω is the rotation rate of the planet, relative to Earth's 1 rotation per day. This can be extended to be time variable, such as having CO_2 emissions increase pressure, change

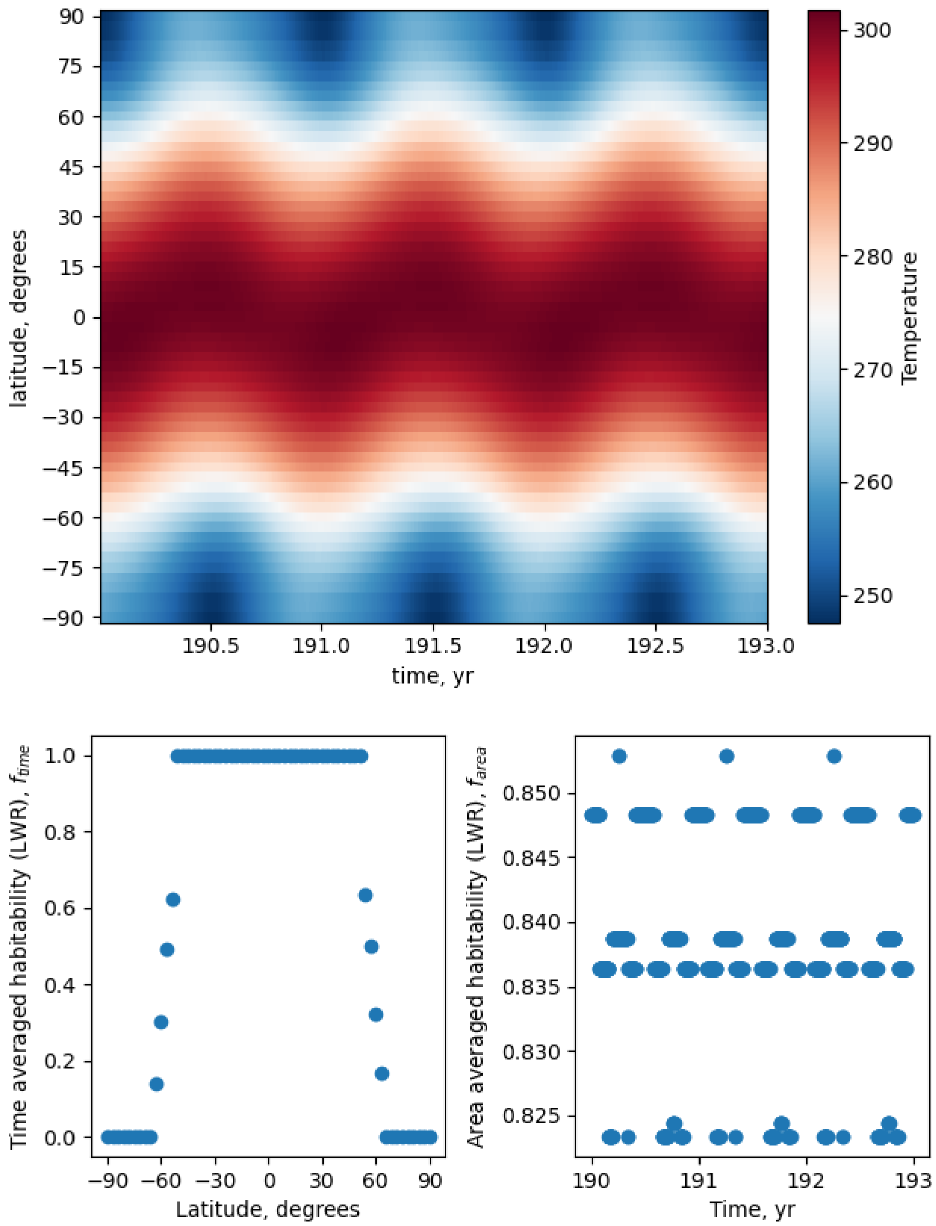

FIG. 2: Top: The temperature distribution for the Earth model with parameters given in Table I. The time range is for 2 years, showing the periodicity of the seasons in the model. Bottom: The temperature distribution processed with the LWR habitability (eqn. (16)) and then averaged over time (left) or area (right).

heat capacity, and increase mass of particles. However this paper only considers varying the rotation rate of the planet.

Heat capacity, $C(\lambda, T)$, varies with latitude through the ocean-land fraction, $f_o(\lambda)$, and with temperature through the ice-ocean fraction, $f_i(T)$, as

$$C(\lambda, T) = (1 - f_o(\lambda))C_{\text{land}} + f_o(\lambda)((1 - f_i(T))C_{\text{ocean}} + f_i(T)C_{\text{ice}}(T)), \tag{21}$$

Where $C_{\text{land}} = 5.25 \times 10^6$ Jm^{-2}K^{-1} and $C_{\text{ocean}} = 40 \times C_{\text{land}}$ are constant, and

$$C_{\text{ice}}(T) = \begin{cases} 9.2C_{\text{land}} & T \geq 263\text{K} \\ 2.0C_{\text{land}} & T < 263\text{K}, \end{cases} \tag{22}$$

which encapsulates the additional energy requirements of the heat of fusion, and expects that the water would be entirely frozen below -10°C. The ratio of ocean to land for the Earth is 70% ocean to 30% land. This model assumes this ratio is uniform and constant across the entire planet, thus $f_{\text{o}} = 0.7$. This is a simplification as the Earth has an uneven distribution of land and ocean, with most of the land in the northern hemisphere.

With definitions of diffusion and heat capacity, the timestep and latitude step which are numerically stable can be calculated. To do this the EBCM is investigated with a plane wave solution and boundaries on the timestep and latitude step are found. The explicit calculation of this is shown in appx. A, with the result that, for constant diffusion and timestep, a lower heat capacity requires a larger latitude step. The default values for the model are then taken as a timestep of $\Delta t = 1$ day and $S = 61$ latitude nodes ($\Delta\lambda = 3°$ separation)/ These parameters give good resolution while being completely numerically stable. For planets with $f_{\text{o}} = 0$ a lower value of $S = 31$ is chosen as it is stable for the land-only heat capacity value.

WK97 provides three sets of IR-emission and Albedo functions. Following the example of SMS08 and Dressing et al 2010 (here on Dressing10) [3] the second set of IR and Albedo functions which are given by

$$I(T) = I_2(T) = \frac{\sigma T^4}{1 + 0.5925(T/273\text{K})^3} \tag{23}$$

$$A(T) = A_2(T) = 0.525 - 0.245 \tanh\left(\frac{T - 268\text{K}}{5}\right), \tag{24}$$

are used in all models. This IR-emission is a blackbody radiation term (numerator) damped by the optical thickness of the atmosphere (denominator) which is roughly equivalent to the greenhouse gas effect due to water vapour content in the air. The albedo function is a smooth scaling from low reflectivity of land and forest to high reflectivity due to ice and snow.

The insolation function, S, is defined in WK97 as the day averaged incident (based on latitude) radiation from the sun,

$$S(\lambda, t) = \frac{q_0}{\pi}\left(\frac{1\text{ au}}{a}\right)^2 (H(t)\sin\lambda\sin\delta(t) + \cos\lambda\cos\delta(t)\sin H(t))$$

where $q_0 = 1360$ Wm^{-2} is the insolation from the Sun, a is the distance from the Sun, $\cos H(t) = -\tan\lambda\tan\delta(t)$ is the radian half-day length with $0 < H < \pi$, and $\delta(t)$ is the solar declination defined by

$$\sin\delta(t) = -\sin\delta_0\cos(L_s(t) + \pi/2)$$

where δ_0 is the obliquity of the planet and $L_s(t) = \omega t$ is orbital longitude from an orbital angular velocity found by Kepler's laws. It is important to average over a day insolation as the model does not have a longitude dimension, so cannot account for uneven distribution of the insolation, for example in the case of a tidally locked planet.

The temperature distribution for the Earth model is shown in Fig. 2 for 2 years after 190 years of evolution. There is clear periodicity in the model corresponding clearly with the seasonal variations experienced by the Earth.

Also shown is the LWR habitability of this temperature data which has been time averaged with eqn. (13) and area averaged with eqn. (12). The total habitability given by eqn. (14) is $H_{\text{Earth}} = 0.84$, meaning that the Earth is, when using LWR, 84% habitable. When using HC habitability this value is slightly reduced but the same to two significant figures.

The time averaged habitability shows how the the equator is habitable all year around. The poles are uninhabitable year round. Between $65°$ to $45°$ the habitability decreases linearly, representative of the variablity of the frost line.

The area averaged habitability changes in steps as each discrete latitude band becomes habitable or uninhabitable. It is periodic but difficult to predict within each year.

5. EARTH-LIKE EXOPLANETS

A. Investigating time-averaged solar flux

General temperature relations for a planet can be found from the 0D EBCM. Time averaged insolation of an planet in an elliptical orbit is given by

$$\langle F \rangle = \frac{q_0}{a^2\sqrt{1-e^2}}, \tag{25}$$

where $q_0 = L_{\text{Sun}}/4\pi a_{\text{Earth}}^2 \approx 1360\ \text{Wm}^{-2}$ is the bolometric solar flux for Earth, a and e are the semimajor axis and eccentricity respectively of the planet [4].

By subsituting this relation into equation (1), the temperature of a planet can be related to semimajor axis and eccentricity through

$$T \propto a^{-\frac{1}{2}}(1-e^2)^{-\frac{1}{8}}, \tag{26}$$

with proportionality constant $(q_0(1-A)/4\sigma)^{1/4} = 255$ K for an Earth-like albedo of 0.3.

The validity of this proportionality can be investigated in terms of the semimajor axis by keeping $e = 0.0167$ constant and varying a from just outside Mercury's orbit at 0.5 au to Mars' orbit at 1.5 au. As seen in Figure 3 there are three main zones of interest to consider.

The first zone with $a < 0.65$ au has temperatures too high to sustain liquid water due to being too close to the Sun. The second zone with $0.65 < a < 1$ au is much more temperate, and is able to sustain liquid water on the planet's surface. Both the first and second zones are described by $\langle T \rangle = p_1 a^{q_1} = 293a^{-0.505}$ which is very close to the expected $a^{-0.5}$ powerlaw seen in eq. (26). The value of p_1 is 38 K higher than the proportionality constant above, most likely due to the additional greenhouse effect present in the 1D model.

The third zone with $a > 1$ au is a sudden departure from this expected powerlaw to $\langle T \rangle = p_2 a^{q_2} = 210.2a^{-0.378}$. This is due to the ice albedo feedback which works as follows. As the planet cools, ice forms with a higher albedo than the land or ocean. This higher albedo means more light is reflected, thus the planet absorbs less heat, so cools more. This cycle continues until the planet reaches a much colder equilibrium than is expected by a fixed albedo method. At

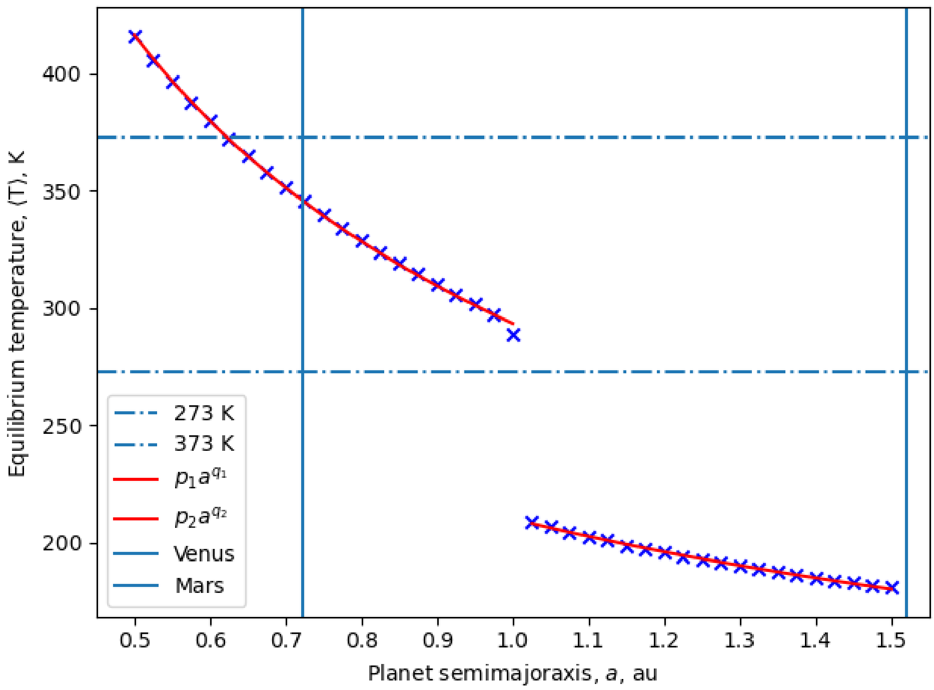

FIG. 3: A plot of the globally averaged temperature of the planet when varying its semimajor axis at constant eccentricity of $e = 0.0167$. Overlaid on the plot are two curves which are fitted to the data by a least squares regression. The form of the curve is $\langle T \rangle = p_i a^{q_i}$. It is expected from a 0D EBCM (see eq. (26)) that $q_i = -0.5$. The first zone obeys the expected powerlaw nicely, with $q_1 = -0.505 \pm 0.004$. The other free parameter for the first zone is $p_1 = 293.5 \pm 0.4$. The "snowball" zone after 1 au represents a sudden drop in temperature due to ice-albedo feedback, and follows a very different powerlaw to the first zone. Free parameters for this zone are $p_2 = 210.2 \pm 0.2$ and $q_2 = -0.378 \pm 0.003$ Also shown are Venus and Mars to highlight the range of values considered.

1 au the planet is on a tipping point in terms of this feedback loop, as seen by the temperature being slightly lower than expected by eqn. (26). This, along with the following analysis of eccentricity and obliquity, help show why the Earth has had many ice ages in the past [5].

Alternatively, a can be fixed at 1 au and the eccentricity can be varied from a perfect circle, $e = 0$, to a very eccentric ellipse, $e = 0.9$. Beyond $e > 0.9$ the iteration to find orbital distance converges much less quickly so becomes intractible. Additionally planets in extreme orbits with $e > 0.9$ would be extremely unstable and most likely would not be able to retain an atmosphere due to extreme temperatures.

Similar to varying the semimajor axis, there are two main zones of interest in Figure 4 where the eccentricity of the planet is varied.

The zone with $e > 0.2$ follows the relationship well, and the globally averaged temperature doesn't exceed the boiling point of water. On the other hand, the zone with $e < 0.2$ is up to 5 K lower than the relationship. This dip is again due to ice albedo feedback. High eccentricities mean the planet gathers and stores enough thermal energy when close to the Sun to prevent polar ice caps from forming even when further away from the Sun. Lower eccentricities allow for polar ice caps to form which then significantly lower the global temperature.

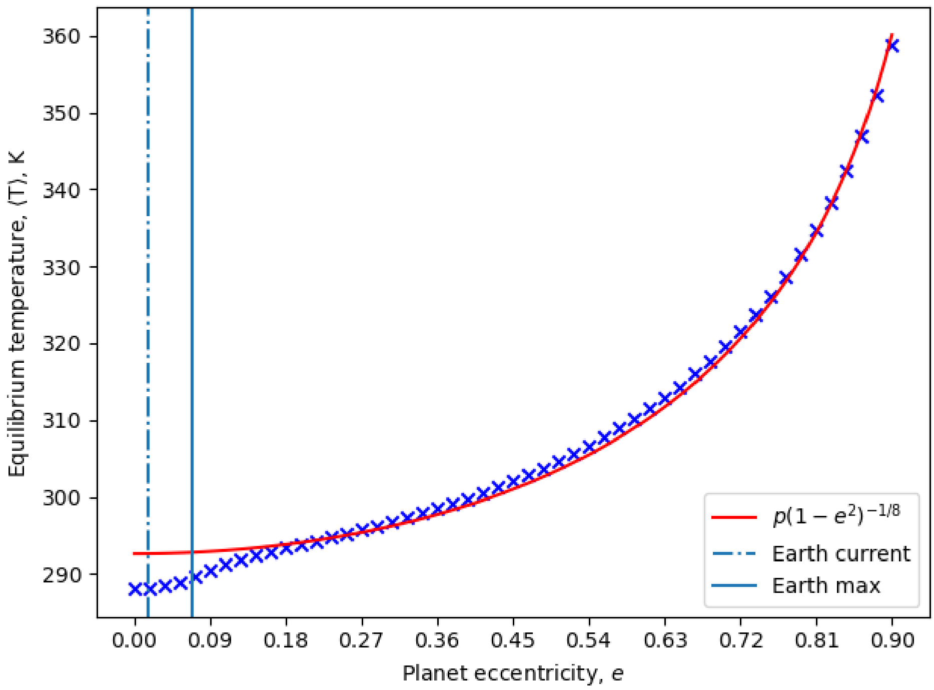

FIG. 4: A plot of the globally averaged temperature of the planet when varying its eccentricity at constant semimajor axis of $a = 1$ au. Overlaid on the plot is a curve which is fitted to the data by a least squares regression. The form of the curve is $\langle T \rangle = p(1-e^2)^{-1/8}$. The proportionality constant $p = 292.6 \pm 0.2$ K, which is higher than expected due to greenhouse effects. Also shown are the current and maximum theoretical value of Earth's eccentricity [6]. The minimum value is 0. There is a large dip at lower eccentricities due to ice albedo feedback forming polar icecaps.

As seen from the vertical lines in Fig. 4, the Earth has moved in this lower eccentricity region for its entire history, suggesting that the presence of the polar caps has been reasonably constant for the recent past.

B. Semimajor axis and eccentricity

C. Obliquity

D. Ocean fraction

6. EXOMOONS

A. Eclipsing

Eclipsing of the moon by the gas giant was initially investigated with two independent 2-body solutions for gravitational attraction which showed that varying the eccentricity of the moon or planet resulted in no change to time-averaged eclipsing fraction. Thus, the main influences of eclipsing are gas giant semimajor axis and moon semimajor axis, with moon semimajor

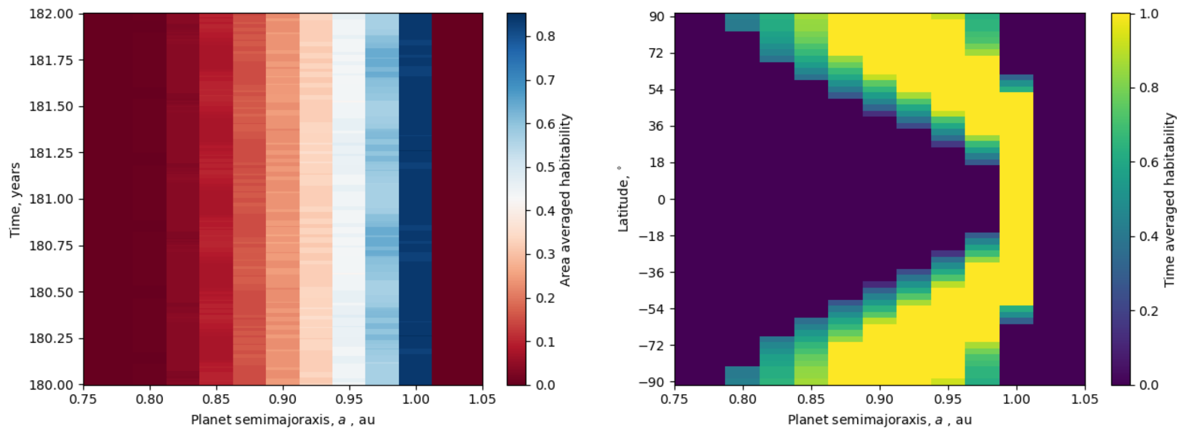

FIG. 5: Left: The area-averaged human habitability for a 2 year period after 180 years of simulation. The planet is never 100% habitable, reaching a maximum of 85% when at the Earth-like 1 au. Cyclical variations in habitability can be seen for $a < 1$ au. This indicates seasonal variation where the planet becomes too cold or, more likely, too hot for the human compatible habitability considered. Right: The 10 year time-averaged human habitability for each latitude band. In this case some latitude bands do reach 100% habitability. Decreasing a from 1 au causes the equator to become too hot for habitability, and melts the ice caps which are then habitable. Increasing a from 1 au causes ice caps to grow and the planet to fall into a snowball state which is too cold for habitability.

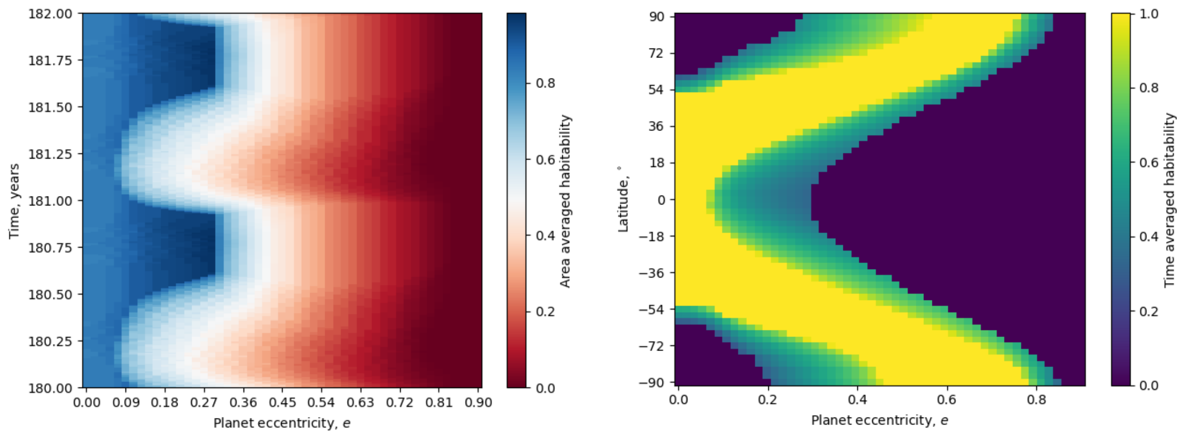

FIG. 6: Left: The area-averaged human habitability for a 2 year period after 180 years of simulation. The planet is never 100% habitable, reaching a maximum of 85%. There is a sharp cut off between $t = 180.5$ and $t = 181$ years where the equator has cooled as the planet is further from the Sun, but is still considered uninhabitable due to exceeding the maximum allowed temperature (40°C). At $t = 180$ years the planet is at perihelion, and is at aphelion at $t = 180.5$ years. Right: The 10 year time-averaged human habitability for each latitude band. As eccentricity increases the habitable zones of the planet move outwards towards the poles which are less directly insolated. Higher eccentricities both melt the poles and cause the equatorial regions to be too hot.

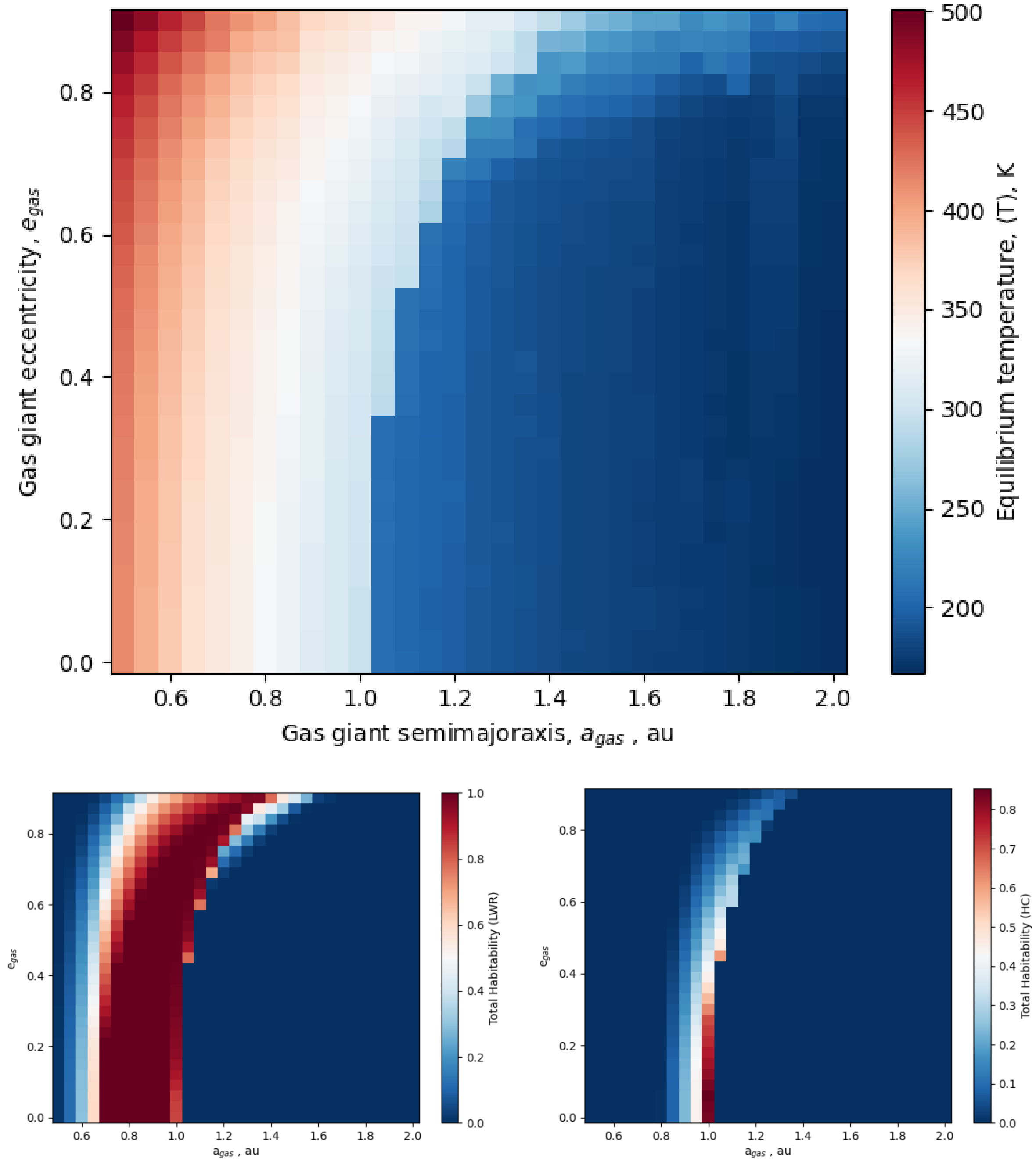

FIG. 7: Top: Varying the semimajoraxis and eccentricity of the gas giant to produce a heat map for the equilibrium temperature of the planet. Left: Processing of the temperature data with eqn. (16) and eqn. (**??**). Right: Processing of the temperature data with eqn. (17) and eqn. (**??**).

axis being the most important factor.

In order to add eclipsing to the EBCM without running the 2-body solution in parallel, the eclipsing fraction must be quantified. To do this the star is assumed to be a point source, and both planets are assumed to be in circular orbits which are coplanar. Figure 10 shows the configuration of the system, including the angle 2α which is the fraction of the moon's orbit which is spent being eclipsed.

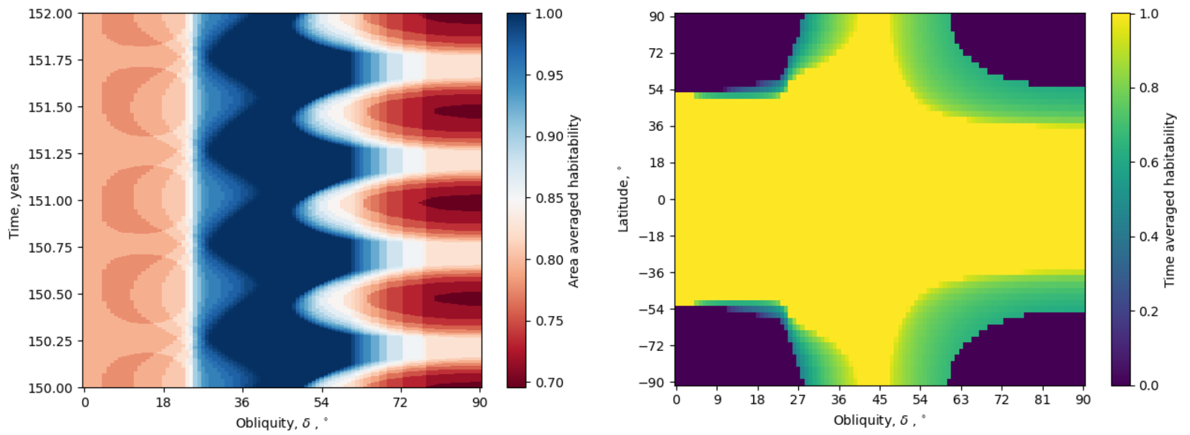

FIG. 8: Left: The area-averaged human habitability for a 2 year period after 150 years of simulation. The habitability varies between 70% and 100%, with the highest habitabilities being between 20°and 50°At lower obliquities polar ice caps form reducing the area habitability. There is a small seasonal variation in the habitability due to these polar ice caps growing and shrinking as they are more or less directly insolated. At high obliquities the variation is more extreme, where the pole being directly insolated melts and then reaches temperatures which are too hot, then the other half of the time are more temperate so can sustain life better. Right: The 10 year time-averaged human habitability for each latitude band. Habitability at the equator of this planet is usually totally habitable all year around. The poles vary from totally uninhabitable from cold, habitable, to partially uninhabitable due to cyclical heating then freezing.

α can be related to the length x by

$$\sin\alpha = \frac{x}{a_{\text{moon}}}, \tag{27}$$

θ can be related to the length x by

$$\sin\theta = \frac{x}{a_{\text{gas}} + a_{\text{moon}}\cos\alpha} = \frac{r_{\text{gas}}}{a_{\text{gas}}}, \tag{28}$$

combining eqns. (27) and (28) leads to

$$(a_{\text{gas}} + a_{\text{moon}}\cos\alpha)\frac{r_{\text{gas}}}{a_{\text{gas}}} = a_{\text{moon}}\sin\alpha, \tag{29}$$

thus

$$\frac{r_{\text{gas}}}{a_{\text{moon}}} = \sin\alpha - \frac{r_{\text{gas}}}{a_{\text{gas}}}\cos\alpha, \tag{30}$$

By approximating $r_{\text{gas}} \gg a_{\text{gas}}$, α can be solved for. Dividing 2α by the full 2π angle the moon rotates through, the eclipsing fraction can be found as

$$\epsilon = \frac{2\alpha}{2\pi} = \frac{\arcsin(R_{\text{gas}}/a_{\text{moon}})}{\pi}, \tag{31}$$

for a planet of radius R_{gas} and moon semimajor axis a_{moon}.

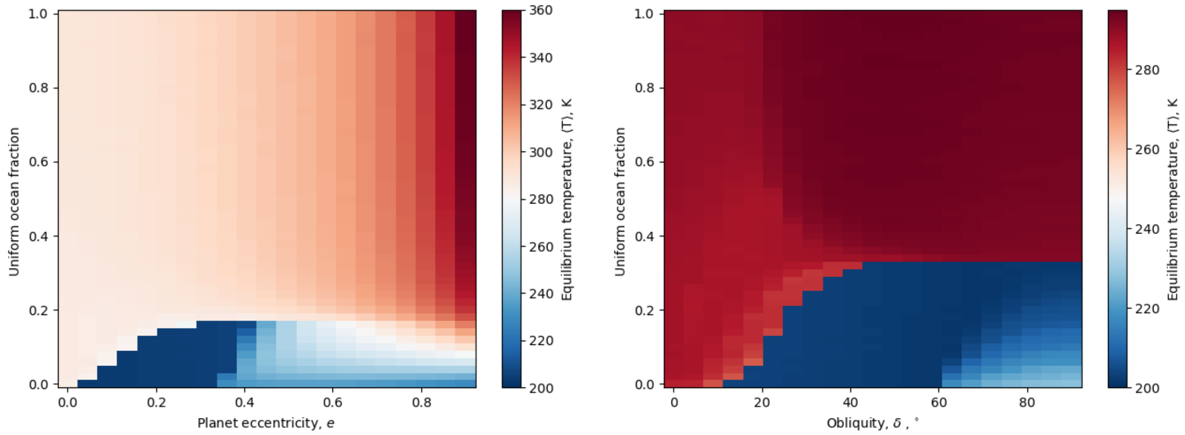

FIG. 9: Graphs show the minimum ocean fraction required to keep the planet thermally stable (i.e. not fall into a snowball state) for different eccentricities (Left) and obliquities (Right) at constant semimajor axis of 1 au. While both temperature scales start at 200 K, the eccentricity graph reaches 360 K whereas the obliquity graph reaches 295 K. Both variables cause the planet to be susceptible to ice-albedo feedback, and both cause full or partial recovery from snowball at extreme values. For eccentricity the minimum ocean fraction varies approximately quadratically with eccentricity until $e = 0.4$ where the eccentricity is high enough to melt the induced snowball meaning the time averaged temperature increases. The minimum ocean fraction in the obliquity case varies with an 'S' shape and levels out after $\delta = 40°$ to a minimum ocean fraction of $f_{\text{ocean, min}} = 0.36$. Similar to the eccentricity case, high obliquities can partially recover from the snowball. In this case it is due to the pole facing the Sun melting for half a year due to constant insolation before refreezing when facing away from the Sun. There are nearly no variations due to changing ocean fraction above $f_{\text{ocean}} = 0.2$ in the eccentricity case, and few variations above $f_{\text{ocean}} = 0.4$ for the obliquity case.

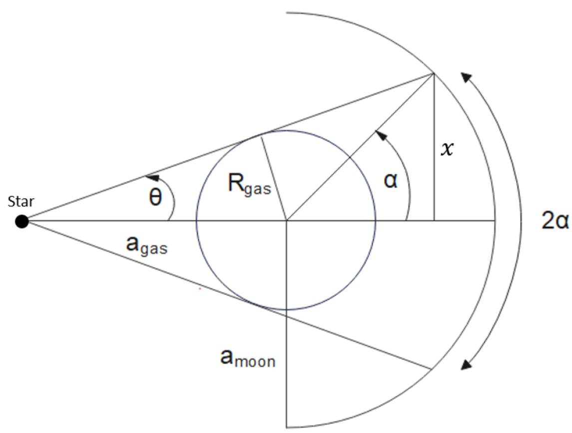

FIG. 10: A diagram of a planet in orbit around a star at a distance a_{gas}, and a moon in orbit of the planet at a distance a_{moon}. The planet has radius R_{gas}. The angle 2θ corresponds to the angular size of the planet from the star. Inside the angle 2α the moon is eclisped by the planet.

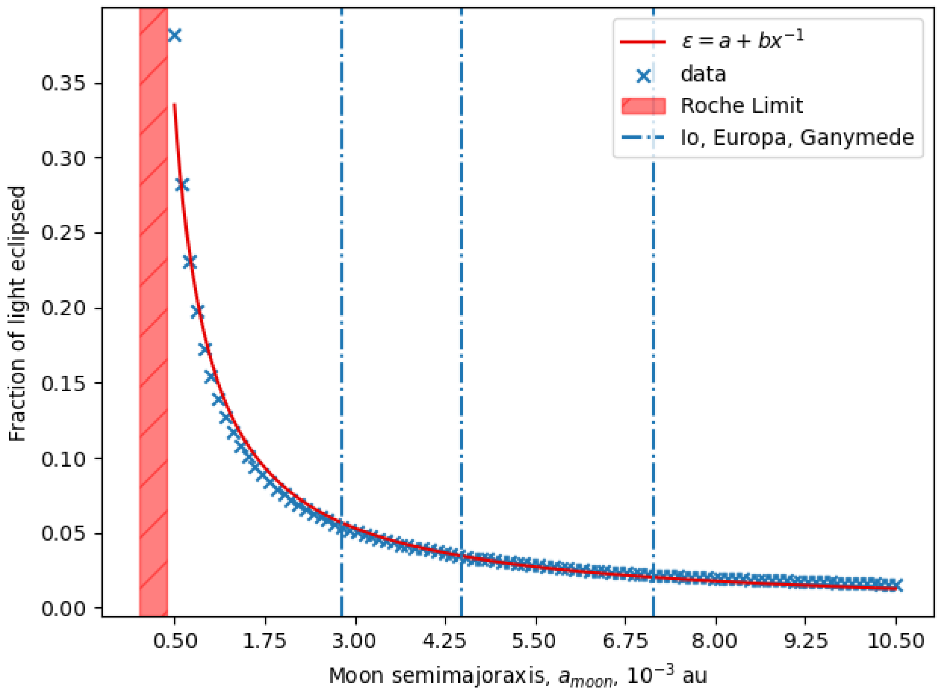

FIG. 11: Fraction of light eclipsed by a Jupiter sized gas giant when varying a moon's semimajor axis. Shown is the Roche limit for Jupiter, as well as the orbital distances of Jupiter's three innermost moons. Overlaid on the data is a fit of $\epsilon = a + b/x$ with parameters $a = (-3.3 \pm 0.8) \times 10^{-3}$ and $b = (1.69 + / - 0.02) \times 10^{-4}$.

This relation is investigated in Fig. 11 where the fit uses that $\arcsin(x) = x$ for small x. The value of $b = (1.69 \pm 0.02) \times 10^{-4}$ is very close to the theory value of

$$\frac{R_{\text{gas}}}{\pi\ 1.5 \times 10^{11}\text{m au}^{-1}} = 1.48 \times 10^{-4}\text{au}, \tag{32}$$

for a planet with $R_{\text{gas}} = 7 \times 10^{7} m$ with a_{moon} in au.

B. Tidal heating

C. Developing and investigating a depth model

7. DISCUSSION

8. CONCLUSION

REFERENCES

[1] North and Coakley, "Differences between seasonal and mean annual energy balance model calculations of climate and climate sensitivity," J. Atmos. Sci., vol. 36, no. 7, pp. 1189–1204, 1979.
[2] Williams and Kasting, "Habitable planets with high obliquities," Icarus, vol. 129, no. 1, pp. 254–267, 1997.

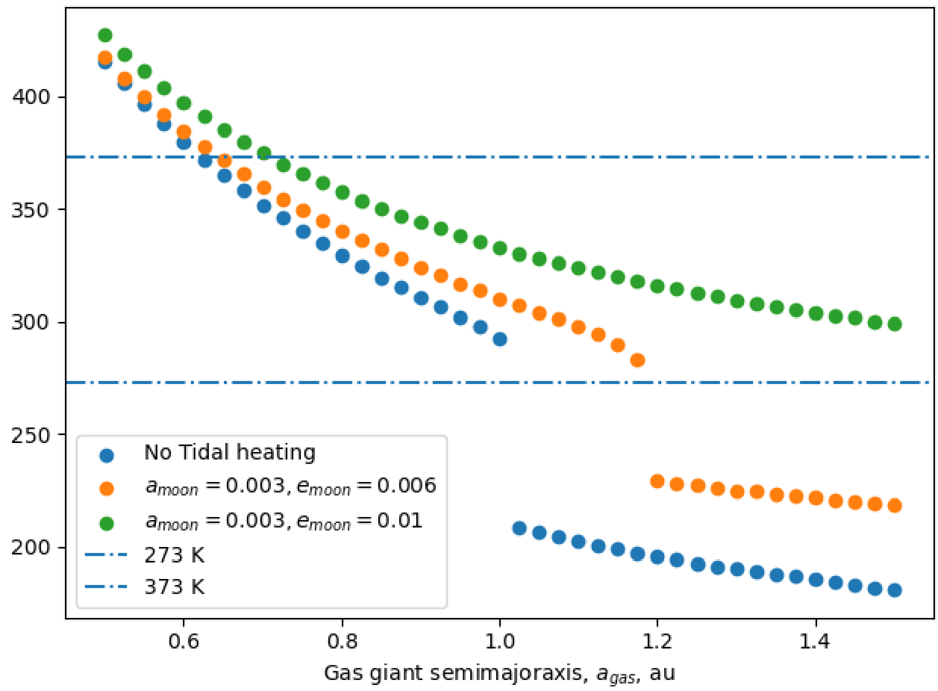

FIG. 12: Qualitative look at how tidal heating effects semimajoraxis temperature curve

[3] C. Dressing and et al, "Habitable climates: the influence of eccentricity," ApJ, vol. 721, no. 2, pp. 1295–1307, 2010.

[4] A. Méndez and E. Rivera-Valentín, "The equilibrium temperature of planets in elliptical orbits," ApJL, vol. 837, no. 1, 2017.

[5] C. Emiliani, "The cause of the ice ages," Earth and Planetary Science Letters, vol. 37, pp. 349–352, 1978.

[6] J. Laskar, A. Fienga, M. Gastineau, and H. Manche, "La2010: a new orbital solution for the long-term motion of the earth," A&A, vol. 532, p. A89, 2011.

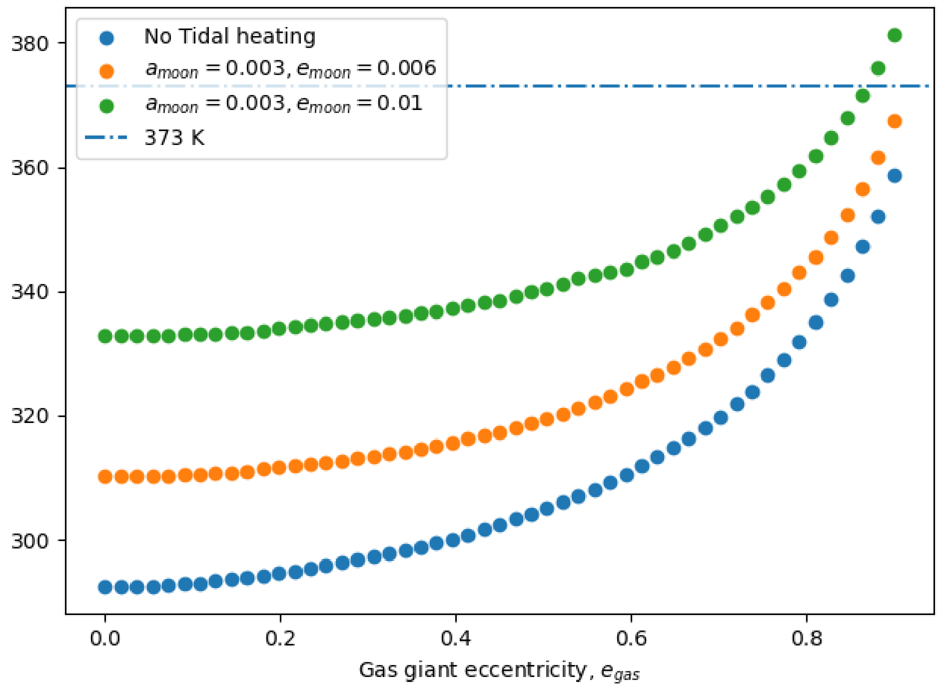

FIG. 13: Qualitative look at how tidal heating effects eccentricity temperature curve

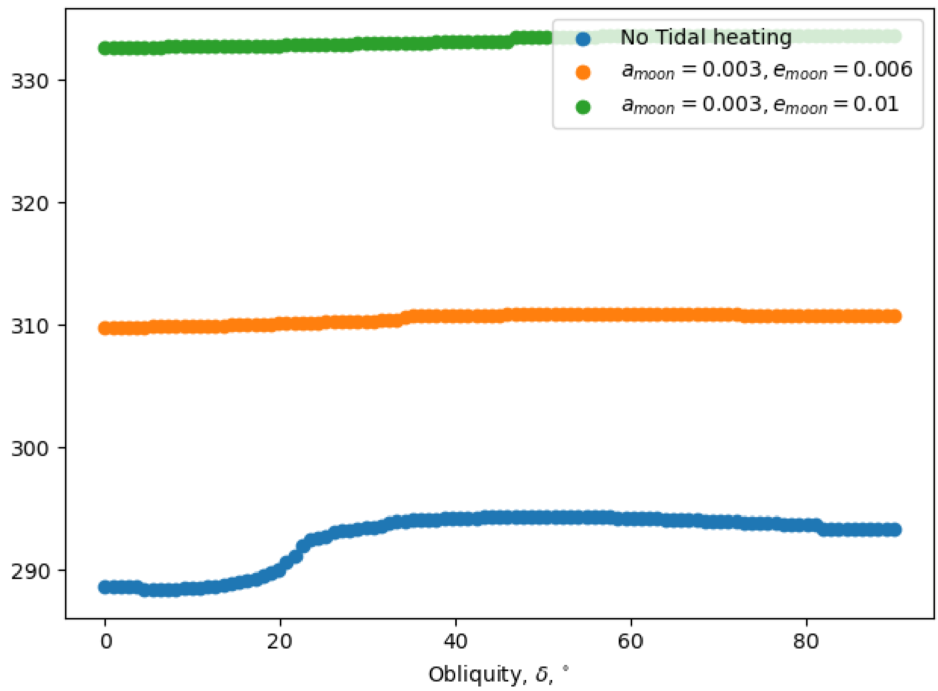

FIG. 14: Qualitative look at how tidal heating effects obliquity temperature curve

Appendix A: Numerical stability of the 1D EBCM

Appendix B: Tidal heating equations and method

SCIENTIFIC SUMMARY FOR A GENERAL AUDIENCE

Many interesting solar systems have been reported in the news, such as the Trappist-1 system which is filled with Earth-like planets. Simulations and models such as those in this paper are used to determine if a planet could be habitable. A habitable zone can be made by varying the parameters of the model to see where the model is habitable, partially habitable, or uninhabitable.

The main model in this paper takes a planet and divides it into a number of latitude bands which can have energy flow between them. Certain parameters, such as how the planet orbits around its star and the angle the planet is tilted at, are varied to build this habitable zone. A result of this paper is if the Earth orbited slightly further away from the Sun then it is likely that it would fall into an ice age similar to what the Earth has experienced in the past. Another result found is that the tilt of the planet can affect how hot or cold it is, and indicates that the current tilt of the Earth gives a cold planet.

Another aspect of this paper's exoplanet research is exomoons orbiting a gas giant such as Jupiter. In certain configurations an exomoon can be heated not only from the host star, but also due to a process called tidal heating. Tidal heating is similar to stretching an elastic band. Stretching and relaxing an elastic band many times can cause the band to warm up. The moon of a gas planet is stretched slightly by unequal forces of gravity as one part of the moon is further away than the other. If the moon's orbit is not circular then the moon is stretched and relaxed, thus heats up in a similar way to the elastic band. Adding tidal heating to the model allows for investigations into how tidal heating can move, or change the shape of, the habitable zone.